

Effect of NiO Loading and Thermal Treatment Duration on Performance of Ni/SBA-15 Catalyst in Combined Steam and CO₂ Reforming of CH₄

Phan Hong Phuong¹, Luu Cam Loc^{1,2,*}, Hoang Tien Cuong² and Nguyen Tri²

¹University of Technology, VNU-HCM, 268 Ly Thuong Kiet Str., HCM City, Vietnam, 70100

²Institute of Chemical Technology VAST, 01 Mac Dinh Chi Str., HCM City, Vietnam, 70100

A series of Ni/SBA-15 catalysts was prepared by impregnation method. Effect of NiO content (30–60 mass%), calcination time (0.5–2 h at 800°C), and reduction time (1–2 h at 800°C) on catalytic performance in combined steam and CO₂ reforming of CH₄ (CSCRM) was studied. N₂ physisorption measurements, powder X-ray diffraction, Hydrogen temperature-programmed reduction, CO₂-temperature-programmed desorption, and transmission electron microscopy were used to investigate physico-chemical properties of the catalysts. The catalytic performance of Ni/SBA-15 in CSCRM was assessed in the temperature range of 550–800°C. The results revealed suitable time for calcination and reduction being 0.5 h and 1.5 h, respectively. After these treatments, 40 mass% NiO/SBA-15 catalyst was more active and exhibited higher activity than others. At 750°C, conversion of CH₄ and CO₂ on this catalyst in CSCRM was 91.05% and 78.11%, respectively. High surface area, better reducibility, and good affinity with CO₂ contribute to the high performance of this catalyst. [doi:10.2320/matertrans.M2018211]

(Received June 29, 2018; Accepted September 14, 2018; Published November 25, 2018)

Keywords: NiO loading, CH₄ reforming, Ni/SBA-15 catalyst, thermal treatment duration

1. Introduction

Emission in greenhouse gases, particularly CH₄ and CO₂, is increasing with high growth rate worldwide resulting in a more serious global warming in our planet. Research on converting these two gases into valuable substances, syngas, by reforming process has been paid much attention. However, CH₄ and CO₂ are stable and reactions to convert these gases require elevated temperature that rapidly deactivates catalysts and also leads to a significantly high cost for the reforming process. Improvement of catalytic performance in reaction converting CH₄ and CO₂ into syngas is mainly based on studying catalysts and adding steam into reaction mixture. In this study, the combined steam and CO₂ reforming of CH₄ to generate synthetic gas was investigated. Metals in VIII B group, especially Ni, Ru, Rh, Pd, Ir, and Pt, have been reported to be highly active in CH₄ reforming processes. Despite higher activity and stability, the usage of noble metals is not preferred due to their high cost and less availability. In general, supported Ni catalysts are commercially being used in steam reforming of CH₄ because of cheap price and fairly good performance compared to the ones with noble metals.^{1,2)} However, coke formation and metal sintering have been making this process inapplicable commercially until recently. Hence, coke resistance improvement of Ni-based catalyst has been attracting attention.

SBA-15 is known as a molecular sieve with large pore size, thick walls, and high thermal resistance.³⁾ Therefore, SBA-15 has commonly been used as a support for dispersing active phase in catalysts, especially those for reaction carried out at high temperature.

Zhang *et al.*⁴⁾ successfully synthesized stable Ni/SBA-15 catalyst for dry reforming of CH₄. Coke deposition onto catalysts leads to deactivation of catalyst with time on stream other than sintering of Ni species. Huang *et al.*³⁾ evaluated catalytic performance of Ni/SBA-15 catalysts promoted by MgO in CSCRM and found that the presence of MgO did not

only improve Ni dispersion through the formation of solid solution but also increase CO₂ affinity. Li *et al.*⁵⁾ indicated that Y₂O₃ enhanced interaction between Ni and SBA-15, resulting in an improvement of Ni dispersion onto the support.

Although SBA-15 is used popularly, the interaction between SBA-15 and active phase is weak due to the inertness of SiO₂ that causes low dispersion of Ni species and sintering of Ni sites with time on stream. Calcination and reduction time are known as two parameters that have a significant effect on improving interaction among active components with support.

To best of our knowledge, impact of calcination and reduction time on activity of Ni/SBA-15 catalyst in CSCRM has not been carried out so far. In this study, effect of these treatment time as well as NiO content in Ni/SBA-15 catalysts on their activity in CSCRM is investigated and optimized.

2. Experimental

2.1 Preparation of catalyst

To prepare SBA-15, 4.0 gram of triblock copolymer P123 was dissolved in 105 gram of distilled water and the obtained solution (I) was stirred for 15–30 minutes. Then, 9.2 mL of Tetraethyl orthosilicate [TEOS-(C₂H₅O)₄Si] was added into solution (I). The mixture was kept stirring for 30 minutes to form solution (II). The following step is to mix and stir 24.3 mL HCl with solution (II) for 30 minutes. Finally, the gel mixture was transferred into a teflon bottle and was aged at 60°C for 24 h. The solid product was then filtered, washed with distilled water, dried at 100°C for 2 h and calcined at 550°C for 10 h in air to obtain SBA-15.

To prepare SBA-15 supported catalysts, NiO was loaded by impregnating of Ni(NO₃)₂ solution on SBA-15 with assistance of ultrasonic at room temperature for 5 h. The NiO content in the catalysts was changed successively, being 30; 40; 50 and 60 mass%. The obtained suspension was stirred regularly at 80°C and 100°C in 2 h for each temperature to vaporize water, and then the sample was calcined in air at

*Corresponding author, E-mail: lclloc@ict.vast.vn

800°C for 0.5–2 h. Before reaction, the catalyst is reduced in 40 mol% H₂/N₂ gas mixture (3 L h⁻¹) for 1–2 h at 800°C.

The catalysts are symbolized as following aNi/SBA-15-b-c, representing NiO content of a mass% loaded onto SBA-15 calcined and reduced at 800°C in b and c hours respectively.

2.2 Characterization

Crystalline structure of the catalysts was determined by X-ray diffraction (XRD) using Bruker D2 Phaser powder diffractometer with CuK α radiation ($\lambda = 0.15406$ nm). Specific surface area of these catalysts was measured on Nova Station B, Quantachrome NovaWin Instrument by the nitrogen adsorption at -196°C . Hydrogen temperature-programmed reduction (H₂-TPR) was carried out on a micro-reactor in a gas mixture of 10 mol% H₂/N₂ at a flow rate of 30 mL min⁻¹ using a Gas Chromatograph GOW-MAC 69-350 with a thermal conductivity detector (TCD). A sample of 50 mg was placed in a quartz tube reactor. Temperature was raised from room temperature to 900°C with a heating rate of 10°C min⁻¹. Morphology of catalysts and particle size of active phase are characterized by transmission electron microscopy (TEM) on FE-SEM JEOL 7401 instrument. The carbon dioxide temperature-programmed desorption (CO₂-TPD) method was used to determine basicity of the catalyst. First, the catalyst was reduced in H₂ at 450°C for 1 h. The system was cooled down to room temperature, followed by CO₂ adsorption at room temperature for 1 h. After purging with N₂ for 1 h at 50°C to remove gas-phase and physically adsorbed CO₂, the sample was heated from 50 to 700°C at a rate of 10°C min⁻¹, and the desorbed CO₂ was also monitored online by using a Gas Chromatograph GOWMAC 69-350 with a TCD.

2.3 Activity test

Activity of the catalysts was tested in a micro-flow reactor under atmospheric pressure at temperature of 550–800°C. A catalyst sample of 0.2 gram with size ranging from 0.25 to 0.5 mm is mixed with an equal volume of quartz. The feed flow rate was 6 L h⁻¹ and concentration of CH₄ in feed stream was 3 mol%. The molar ratio of CH₄:CO₂:H₂O in feed was 3:1.2:2.4. The reaction mixture was analyzed on the Agilent 6890 Plus Gas Chromatograph (HP-USA) using both TCD detector (capillary column HP-PLOT Molesieve 5A) and flame ionization detector (capillary column DB624).

3. Results and Discussions

3.1 Physicochemical characteristics of materials

XRD pattern of SBA-15 in Fig. 1 showed the presence of diffraction peaks at $2\theta = 0.9^\circ$, 1.6° , and 1.84° which characterize the hexagonal regularity of the porous structures of SBA-15.^{6,7} The TEM images in Fig. 2 also confirmed morphology of highly ordered hexagonal pores with long channels of SBA-15 support in the catalysts.⁸ In 40Ni/SBA-15-0.5-0 catalyst, the diffraction peak at $2\theta = 0.9^\circ$ shifted to higher value ($2\theta = 1.1^\circ$) indicating structural order of SBA-15 was decreased. Grafting NiO onto SBA-15 and/or changes occurring in preparation of catalyst could be responsible for this decline in the ordering of the mesoporous structure of SBA-15.

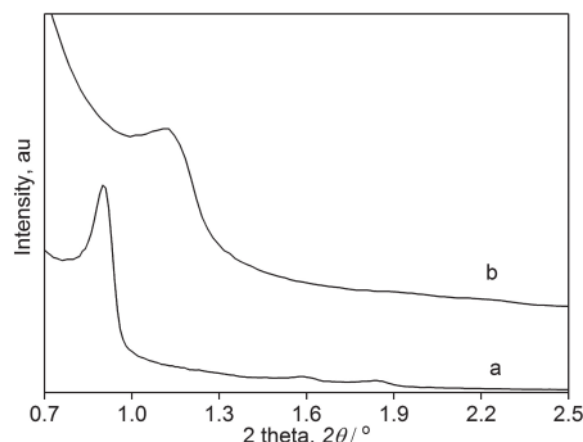


Fig. 1 XRD patterns of (a) SBA-15 and (b) pre-calcined 40Ni/SBA-15-0.5-0 catalyst.

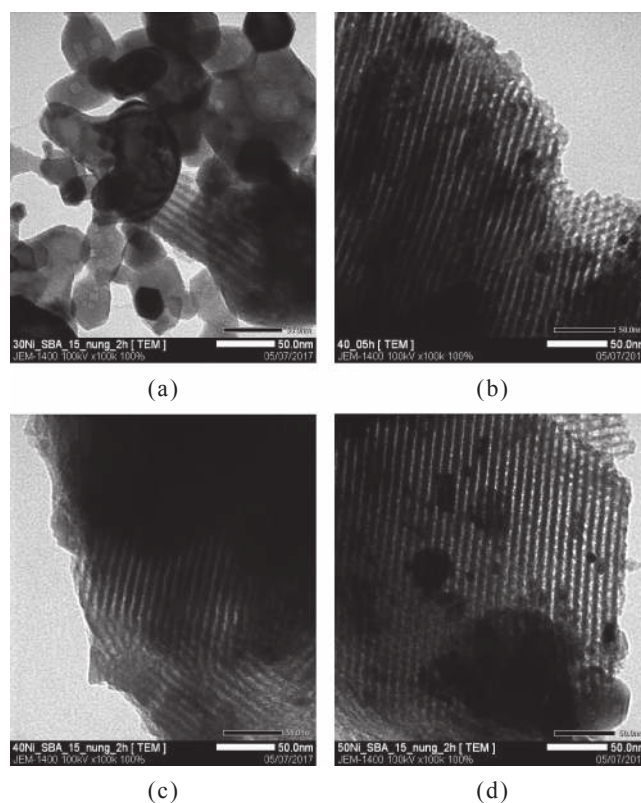


Fig. 2 TEM images of different catalysts; (a) 30Ni/SBA15-2-0. (b) 40Ni/SBA15-0.5-0. (c) 40Ni/SBA15-2-0. (d) 50Ni/SBA15-2-0.

The TEM images showed that there were two types of NiO particles existing on the SBA-15 support, namely NiO particles located inside the pores with a size of a few nm and NiO particles deposited outside the pores having large and various size. The interaction of the NiO particles with SBA-15 could also be accounted for the diffraction peak shift in XRD pattern of the catalysts.

Figure 3 showed the XRD patterns of NiO/SBA-15 catalysts with different NiO loading calcined for 2 h at 800°C. It was found that diffraction peaks with high intensity appeared at $2\theta = 37.3^\circ$, 43.2° , 62.9° , 75.4° , 79.3° corresponding to (101), (012), (220), (311) and (222) plans of face-center cubic crystalline NiO structure in all catalysts.^{9,10} This fact indicated that NiO in all catalyst had a high degree

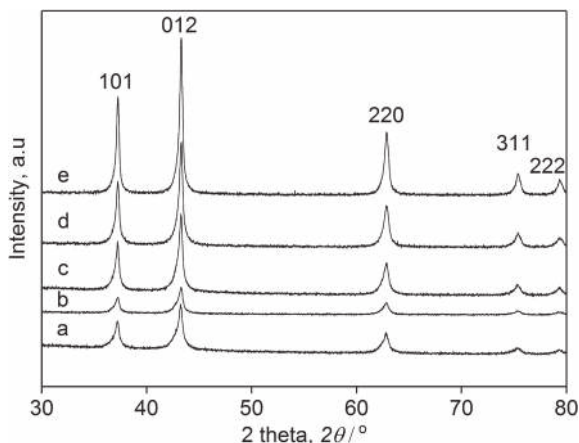


Fig. 3 XRD patterns of pre-calcined Ni/SBA-15 catalysts; (a) 30Ni/SBA15-2-0. (b) 40Ni/SBA15-0.5-0. (c) 40Ni/SBA15-2-0. (d) 50Ni/SBA15-2-0. (e) 60Ni/SBA15-2-0.

of crystallinity. Moreover, these peaks were broader and their intensity increased as NiO content was raised from 30 to 60 mass%, indicating the independent existence of NiO particles on the support surface.

It could be asserted from Fig. 3 that calcination time influenced on structure of catalyst, more specifically, intensity of NiO crystalline peak and its dispersion onto SBA-15 support. Comparing to 40Ni/SBA-15-2-0, intensity of NiO peaks were weaker in 40Ni/SBA-15-0.5-0 catalyst indicating the smaller crystallite size of NiO. This could be explained by the fact that longer time of calcination induced restructuring and metal sintering on the support. Hence, calcination time influenced strongly on crystalline structure and this, in turn, might effect on catalytic performance in reforming process. The NiO crystallite size of NiO/SBA-15-2-0 catalysts calculated by Scherrer equation increased from 12.91 nm up to 18.35 nm when NiO content was raised up from 30 to 40 mass%.

It was followed from the results in Fig. 4 that the BET surface area (S_{BET}) of the catalysts was quite large, ranging from 186 to 230 $\text{m}^2 \text{g}^{-1}$. However, this value was much lower than that of SBA-15 carrier, determined to be approximately

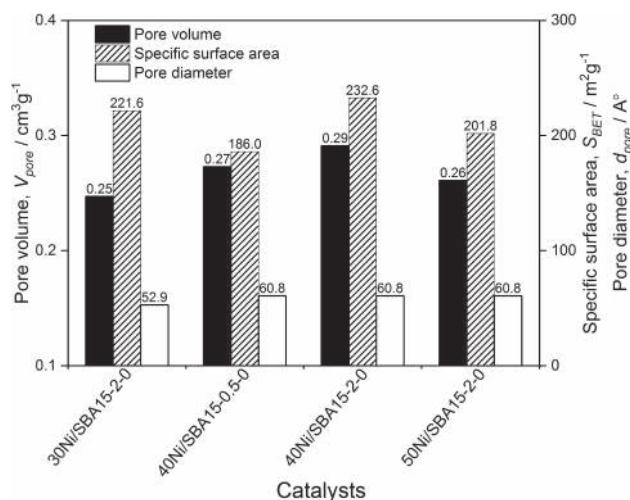


Fig. 4 Pore volume, pore diameter and specific surface area of catalysts.

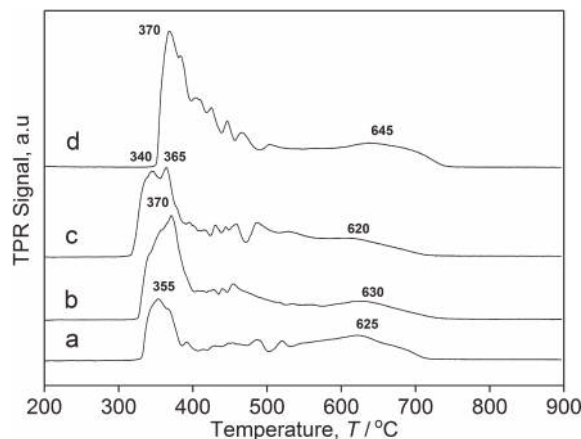


Fig. 5 H_2 -TPR profiles of catalysts; (a) 30Ni/SBA15-2-0. (b) 40Ni/SBA15-0.5-0. (c) 40Ni/SBA15-2-0. (d) 50Ni/SBA15-2-0.

$600 \text{ m}^2 \text{g}^{-1}$. This could be explained by the small specific surface area of NiO and the covering the pores and surfaces of SBA-15 by NiO particles,^{11,12} as observed in TEM images (Fig. 2). As seen in the Fig. 4, catalysts were mesoporous materials with a pore diameter of 5.3–6 nm. The specific surface area of the catalyst, calcined for 2 hours, was greater than that of sample calcined for 0.5 h. In particular, the 40Ni/SBA-15-2-0 catalyst had the biggest pore volume ($0.291 \text{ cm}^3 \text{g}^{-1}$) and specific surface area ($232.6 \text{ m}^2 \text{g}^{-1}$).

H_2 -TPR profiles of Ni/SBA-15 catalysts with different NiO content were shown in Fig. 5. Obviously, all catalysts showed peaks in the temperature range of about 300–500°C and one peak at 520–720°C. The first peak with high intensity and big area was due to the reduction of NiO clusters, weakly interacting with SBA-15 support. Meanwhile, the second peak with weak intensity could be attributed to the reduction of strongly interactive NiO species with SBA-15 support¹³ or reduction of small clusters of NiO in pores.¹⁴ However, combined with TEM images, it could be suggested that the first reduction peaks were attributed to the reduction of NiO cluster locating outside, while the second one characterized the reduction of NiO particles existed in the pores of SBA-15. As NiO content was increased, the reduction peaks shifted toward higher temperature and higher consumption of H_2 was observed. This might be related to an increase in particle size as the NiO content increases (as observed from XRD and TEM results).

Increasing in calcination time led to a decrease in area of reduction peak. Typically, 40Ni/SBA-15-2-0 catalyst had smaller area of reduction peak than 40Ni/SBA-15-0.5-0 did. This could be explained by the fact that longer time of calcination induced sintering of active component on the support.

Hence, it could be deduced that amount of NiO as well as calcination time greatly influenced on catalysts' reducibility contributing probably to an improvement of catalytic performance.

CO_2 -TPD results in the Fig. 6 reflected that catalysts with different amount of NiO exhibited different strength of basicity. It could be seen that there were two desorption peaks in CO_2 -TPD pattern appearing at 60–250°C and 450–600°C, corresponding to weak and moderate basic sites.³ These

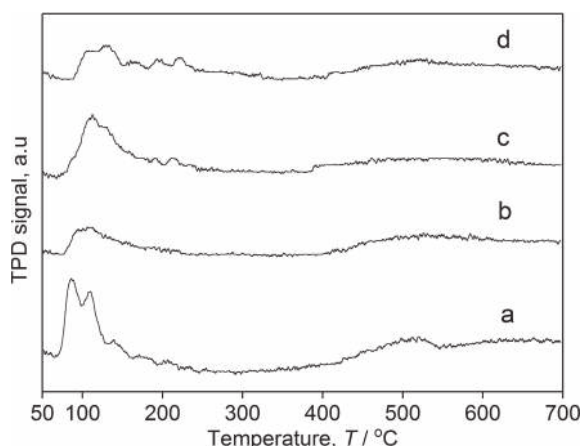


Fig. 6 CO_2 -TPD patterns of Ni/SBA-15 catalysts; (a) 30Ni/SBA15-2-0; (b) 40Ni/SBA15-2-0; (c) 40Ni/SBA15-0.5-0; (d) 50Ni/SBA15-2-0.

peaks shifted to higher temperature with increasing of NiO loading from 30 to 40 mass% indicating a stronger CO_2 affinity of 40Ni/SBA-15 catalyst. When NiO content was raised from 40 to 50 mass%, desorption peaks increased in area without shifting temperature. This fact showed the presence of more basic sites with similar strength when there was a bigger amount of NiO. Besides, increasing in calcination time led to smaller area of CO_2 desorption peaks corresponding to weaker ability to absorb CO_2 and less base sites. This indicated that the basicity of 40Ni/SBA-15-2-0 was weaker than of 40Ni/SBA-15-0.5-0 contributing possibly to a higher conversion of CO_2 in CSCRM on second catalyst than on the first one.

3.2 Catalytic activity of materials

3.2.1 Effect of NiO loading

Figure 7 showed CH_4 and CO_2 conversion in CSCRM over Ni/SBA-15 catalysts with NiO content varying from 30 to 60 mass%. 30Ni/SBA-15-2-2 catalyst had the lowest activity among tested catalysts. This was consistent with what was observed in H_2 -TPR pattern that showed fewer amounts of ions Nickel reduced on the support. Besides, although there was a bigger amount of basic sites, strength of these sites of 30Ni/SBA-15-2-2 was weaker comparing to other catalysts. This was accounted for a lower CO_2 conversion on the 30Ni/SBA-15-2-2 catalyst. When NiO content in the catalyst was raised up from 30 to 40 mass%, CH_4 conversion was enhanced. However, CH_4 conversion on the catalysts remained unchanged ($\sim 90\%$) at reaction temperature from 700 to 800°C when NiO content was increased from 40 to 60 mass%. Metal sintering due to bigger amount of NiO in the catalyst might be the reason for these facts.

3.2.2 Effects of calcination and reduction duration

Effect of calcination time, up to 2 h, on catalytic activity in CSCRM is shown in Fig. 8. Both CH_4 and CO_2 conversions were enhanced as reaction temperature rose up because CSCRM reaction was strongly endothermic. However, these conversions did not change considerably when the temperature increased in the interval of 650 – 800°C . This might be because the fact that carbon and CO_2 could be produced from CO by Boudouard reaction.

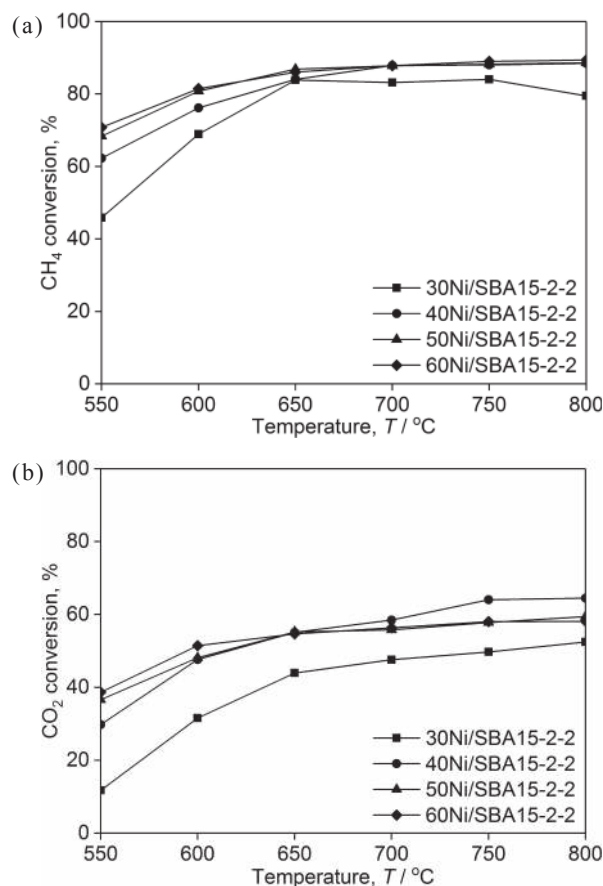


Fig. 7 CH_4 (a) and CO_2 (b) conversion on Ni/SBA-15 catalysts at different temperatures.

The 40Ni/SBA-15-0.5-2 catalyst had good conversions even at low reaction temperature (650°C). The best catalytic activity of 40Ni/SBA15-0.5-2 could be explained by its TPR patterns. Increase in calcination temperature could lead to sintering of active phase, resulting in a less amount of active component after reduction. Besides, it could be deduced from CO_2 -TPD results that more basic sites were present in 40Ni/SBA-15-0.5-2 catalyst contributing to a higher CO_2 affinity and CO_2 conversion, as a result. Hence, calcination time for 0.5 h is the optimum value for Ni/SBA-15 catalyst in CSCRM in the tested region of calcination time.

Figure 9 showed the catalytic activity of Ni/SBA-15 catalysts reduced for different time in CSCRM. It could be seen that, both CH_4 and CO_2 conversion increased when reaction temperature was raised up. In addition, the catalytic activity of 40Ni/SBA-15-0.5-1.5 and 40Ni/SBA-15-0.5-2 were not much different at reaction temperature in the interval of 650 – 800°C and being better than that on 40Ni/SBA-15-0.5-1. Moreover, molar ratio of H_2 :CO in the product mixture fluctuated from 2.0 to 2.3, being almost consistent with the stoichiometry of CSCRM. Therefore, suitable reduction time among tested value was 1.5 h.

4. Conclusion

Calcination duration strongly contributed to physicochemical properties of the catalyst. An increase in calcination time might cause sintering of metal species leading to a decrease

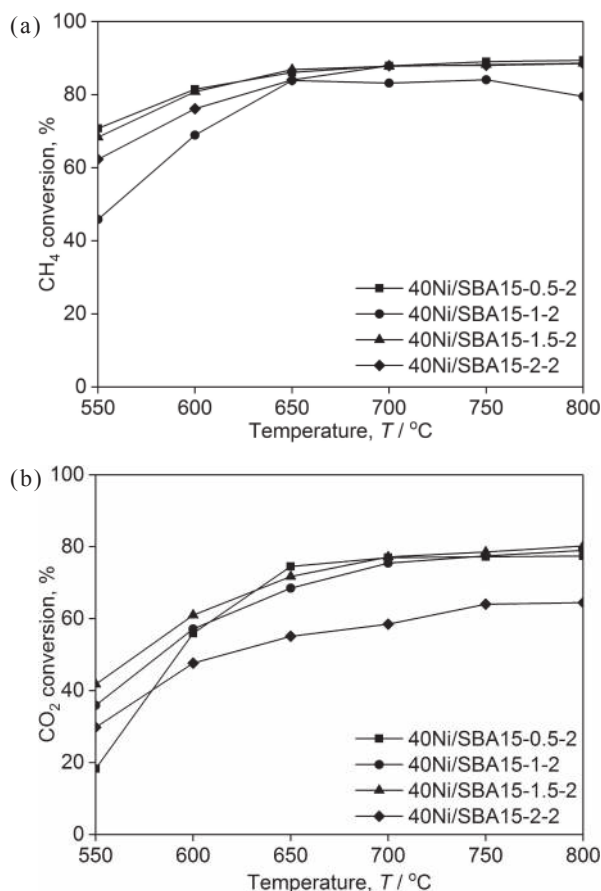


Fig. 8 CH₄ (a) and CO₂ (b) conversion on 40Ni/SBA-15 catalysts with different calcination duration.

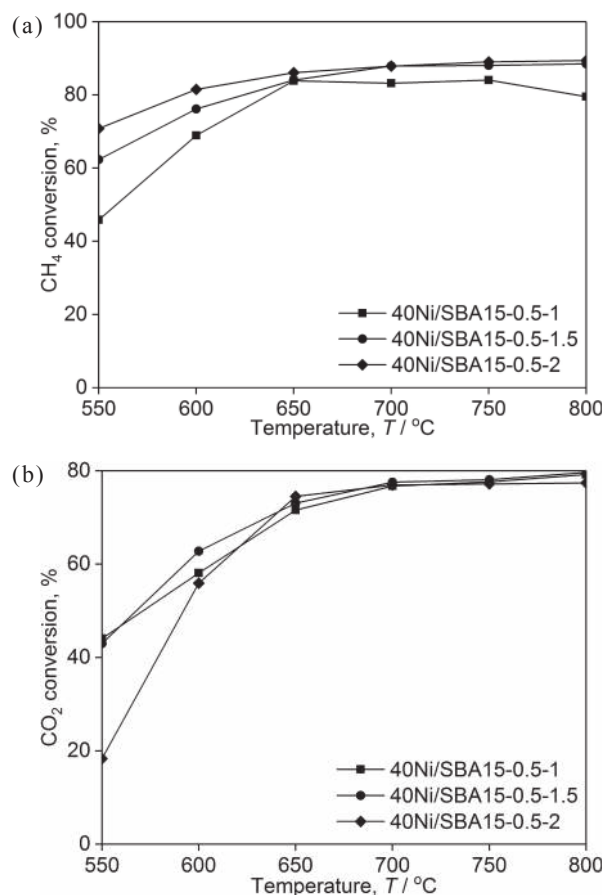


Fig. 9 CH₄ (a) and CO₂ (b) conversion of 40Ni/SBA-15 catalysts with different reduction duration.

in catalytic activity in CSCR. The activity of catalyst was also affected by reduction time. A shorter reduction time might not produce a sufficient active phase on the support while a longer reduction time would lead to a higher cost of production. Hence, the suitable duration of calcination and reduction of catalyst is 0.5 h and 1.5 h, respectively.

The highest activity was observed on the 40Ni/SBA-15-0.5-1.5 catalyst among tested ones for CSCR due to its better reducibility, high CO₂ adsorption and Ni dispersion on the support. On this catalyst, the conversion of CH₄ and CO₂ at 750°C was 91.05% and 78.11%, respectively.

Acknowledgments

This research is funded by The Incubator for Young Science and Technology Program organized by HCM City Department of Science and Technology and HCM City Youth Union in 2018.

REFERENCES

- 1) H.-S. Roh, K.-W. Jun, S.-C. Baek and S.-E. Park: *Catal. Lett.* **81** (2002) 147–151.
- 2) G. Zhang, L. Hao, Y. Jia and Y. Zhang: *Int. J. Hydrogen Energy* **40** (2015) 12868–12879.
- 3) B. Huang, X. Li, S. Ji, B. Lang, F. Habimana and C. Li: *J. Nat. Gas Chem.* **17** (2008) 225–231.
- 4) M. Zhang, J. Shengfu, H. Linhua, Y. Fengxiang, L. Chengyue and L. Hui: *Chin. J. Catal.* **27** (2006) 777–781.
- 5) J. Li, C. Xia, C. Au and B. Liu: *Int. J. Hydrogen Energy* **39** (2014) 10927–10940.
- 6) D. Zhao, J. Feng, Q. Huo, N. Melosh, G.H. Fredrickson, B.F. Chmelka and G.D. Stucky: *Science* **279** (1998) 548–552.
- 7) D. Zhao, Q. Huo, J. Feng, B.F. Chmelka and G.D. Stucky: *J. Am. Chem. Soc.* **120** (1998) 6024–6036.
- 8) M.I.B. Othman: Master Thesis, University Malaysia Pahang, (2014).
- 9) H.D. Setiabudi, N.S.A. Razak, F.R.M. Suhaimi and F.N. Pauzi: *Malaysian J. Catal.* **1** (2016) 1–6.
- 10) Q. Zhang, M. Wang, T. Zhang, Y. Wang, X. Tang and P. Ning: *RSC Adv.* **5** (2015) 94016–94024.
- 11) A.N. Martínez, C. López, F. Márquez and I. Díaz: *J. Catal.* **220** (2003) 486–499.
- 12) M. Aziz, A. Jalil, S. Triwahyono and M. Saad: *Chem. Eng. J.* **260** (2015) 757–764.
- 13) H. Zhang, M. Li, P. Xiao, D. Liu and C.-J. Zou: *Chem. Eng. Technol.* **36** (2013) 1701–1707.
- 14) D. Li, L. Zeng, X. Li, X. Wang, H. Ma, S. Assabumrungrat and J. Gong: *Appl. Catal. B* **176** (2015) 532–541.